PHYSICS AND NEUTRON SCIENCES

Seed Money Fund

In Situ Characterization of Transformation Kinetics in Nickel-Base Superalloys—Developing Methodology to Control Microstructure Evolution

S. S. Babu,[1] D. Q. Wang,[2] and E. A. Payzant[1]
[1]*Metals and Ceramics Division*
[2]*Formerly at the M&C Division, presently at Nomos Corporation, Sewickley, PA 15143*

The goal of the project was to devise new methodologies to track phase transformation kinetics in nickel-base superalloys. With these methodologies, one can evaluate microstructural models, as well as develop new thermal treatments to control microstructure in these alloys. For the first time, the phase transformations in nickel-base superalloys were measured in situ using neutron diffraction with a time resolution of 1 to 2 min. The results showed that the change in lattice misfit between γ and γ′ phases during high-temperature aging depends on the initial microstructure. The results are the evidence for the proof-of-concept that in-situ neutron diffraction using spallation neutron sources can be successfully applied to characterize phase transformations in complex structural alloys.

Introduction

Design, control, and stability of microstructure are essential for achieving excellent high-temperature properties in nickel-base superalloys.[1] The high-temperature strength of these alloys is related to the presence of coherent, hard γ′ ($L1_2$-ordered) precipitates within the γ (face-centered cubic crystal structure) matrix (Fig. 1). The important microstructural parameters are volume fraction, size, shape, and composition of γ′ phase, as well as lattice mismatch between γ′ and γ phases. The above parameters are affected by the bulk composition, heat treatment temperature, and time.[2]

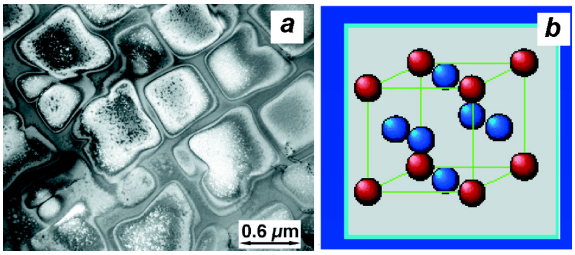

Fig. 1. (a) Transmission electron micrograph from a commercial nickel-base superalloy showing the presence of cuboidal γ′ precipitates within γ matrix. (b) Schematic illustration of crystal structure of $L1_2$-ordered γ′ phase (Ni_3Al) in a binary Ni-Al system (blue atoms correspond to nickel atoms and red atoms correspond to aluminum atoms).

Traditionally, the microstructural control of these alloys is achieved by a trial-and-error approach that includes a change in alloying element concentration and multi-step complex heat treatments. This approach is aided by analyses with differential scanning calorimetry, X-ray and neutron diffraction, and microstructural characterizations using analytical electron microscopy and atom-probe field ion microscopy. Earlier research on simple nickel-base superalloys (Ni-Al-Cr system) showed that the microstructural evolution is related to interactions between phase stability and transformation kinetics.[3] For example, the γ′ precipitates can form by a nucleation and growth mechanism under slow cooling conditions. However, under rapid cooling conditions, the congruent ordering and phase separation may set in, leading to complex microstructural morphology. Extensions of these concepts to multicomponent (Ni-Al-Cr-Ti-Mo-Ta-W system) nickel-base superalloys are limited due to a lack of knowledge on thermodynamic interaction of various alloying elements.[4] Therefore, there is a need to develop methodologies to track phase transformations in these complex alloys using in situ characterization techniques. The results from these measurements will enable us to develop theoretical models that describe the fundamental physical processes that occur during processing of nickel-base superalloys.

The experimental techniques, including differential scanning calorimetry, dilatometry, resistivity, and diffraction measurements using X rays and neutrons, are capable of in situ measurement of transformation kinetics. However, the diffraction technique is superior to other techniques, since it can directly measure the pretransformation events in the γ phase and transformation kinetics of the γ′ phase, including the lattice misfit between γ and γ′ phases. Therefore, the objective of this research was to characterize phase transformations in a nickel-base superalloy using in-situ neutron and synchrotron diffraction technique during high-temperature treatment.

Technical Approach

The main challenge of tracking phase transformation kinetics in nickel-base superalloys using diffraction technique is the required counting time for obtaining a reasonable diffraction spectrum. In conventional X-ray or neutron diffraction techniques for obtaining a reasonable diffraction spectrum, the counting time is on the order of 10 min or more compared with transformation events that are on the order of 1 min or less. Therefore, we need to use high-intensity X-ray sources or high-flux neutron sources with advanced diffraction instruments that are capable of tracking phase transformation event with good time resolution.

In the current research, we used the nickel-base superalloy CM247CC (Ni - 8Cr - 9Co - 5.5Al - 0.8Ti - 0.1Nb - 0.6Mo - 3.2Ta - 9.5W - 0.08C wt. %). The in situ diffraction measurements were made during two experiments. In the first experiment, the alloy with a nonequilibrium microstructure [see Fig. 2(*b*)], obtained by solutionizing at 1290°C for 5 min followed by quenching in water was heated in situ to 1000°C and held at that temperature for 5 h while data was collected at 1-min intervals. The aim of this experiment was to record the structural changes during equilibration of this microstructure.

In the second experiment, the as-received sample [see Fig. 2(*a*)] was heated to 1190°C (i.e., near the solutionizing temperature), cooled to 1000°C at the rate of 0.018°C·s^{-1}, and held at 1000°C for 5 h. The aim of this experiment was to measure the structural changes during the formation of equilibrium γ′ precipitates and during isothermal aging of this microstructure.

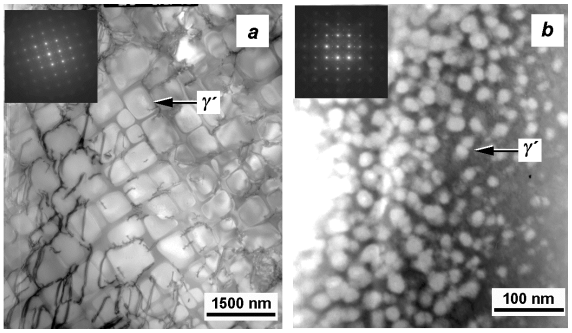

*Fig. 2. Transmission electron micrographs of (*a*) as-received sample showing the microstructure containing cuboidal γ′ precipitates within the γ matrix and (*b*) nonequilibrium microstructure of CM247CC alloy attained by water quenching from solutionizing temperature.*

In the first task, in situ neutron diffraction experiments were performed using the GEM[4] diffractometer (see Fig. 3) at ISIS, UK. The high intensity of the incident beam and the large number (3820) of detectors made it possible to obtain an individual diffraction spectrum of sufficient

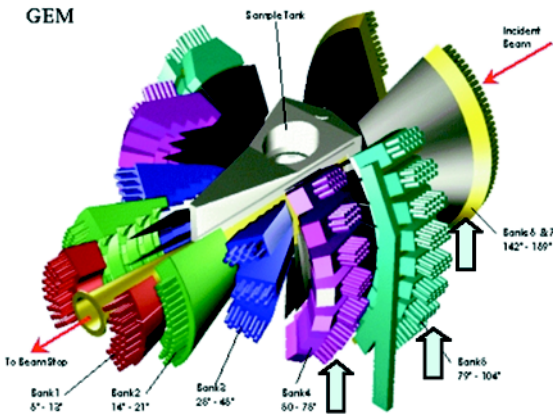

Fig. 3. Schematic illustration of GEM instrument at ISIS facility showing the location of various detector banks, sample tank, and the direction of the incident neutron beam. The arrows show the location of detector banks used in the current experiment.

resolution in 1 min. Since the GEM instrument is based on time-of-flight technique, this allowed for the measurement of diffraction peaks over wide range of d-spacings and scattering angles. In this experiment, diffraction spectra were collected using three banks of detectors placed nominally at 63.6°, 91.3°, and 154.4° in 2θ (see Fig. 3). The samples were 8 mm in diameter and 45 mm long. The heat treatments were performed in situ using a Risø furnace mounted on the GEM diffractometer. The samples were suspended within the heating column using tantalum wire mesh. The temperature control was within ±2°C.

In the second research task, in situ synchrotron diffraction experiments were performed in X-ray beam line X14A at the National Synchrotron Light Source. The samples were in the form of thin strips mounted on a resistance-heating setup that was placed in an atmosphere-controlled chamber. The chamber with the heating setup was mounted on the θ-2θ scanning diffraction instrument. The diffraction measurements were obtained at different angular and time resolution. Due to the limitation of scanning velocity and the need to get good angular resolution, a time resolution of less than 5 min was not achieved.

Results and Accomplishments

The quality of neutron diffraction spectra allowed for whole pattern analyses using the GSAS program,[6] which is based on the Rietveld refinement method. From the data analyses we obtain the relative amounts of γ′ phases and the lattice mismatch between γ and γ′ phases. The lattice mismatch is defined as

$$\delta = \frac{(a_{\gamma'} - a_{\gamma}) \times 10^6}{a_{\gamma}} , \qquad (1)$$

where $a_{\gamma'}$ is the lattice parameter of γ′ phase and a_{γ} is the lattice parameter of the γ phase.[7]

The results from the first experiment are shown in Fig. 4. The typical error for the lattice mismatch was ±70. The lattice mismatch was found to change from ~400 to ~800 while the sample was held at 1000°C. In the same period, the (110) peak intensity of γ′ did not change significantly. These results indicate that there was no growth or dissolution of γ′ phase at this temperature and only changes in the lattice mismatch occurred due to diffusion of alloying elements between γ and γ′ precipitates.

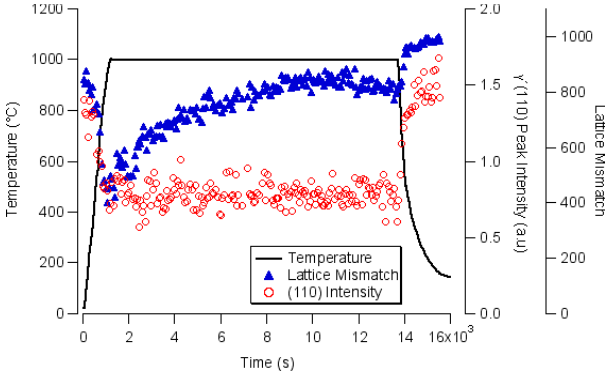

Fig. 4. Measured lattice mismatch between γ and γ′ phases, γ′ (110) peak intensity, and temperature with time from water-quenched sample heated to 1000°C and held at that temperature for 5 h.

The results from the second experiment are shown in Fig. 5. In this case, as the sample was heated to 1190°C, the (110) peak intensity of γ′ phase decreased rapidly, which suggests nearly complete dissolution of γ′ precipitates. The data analyses for the region in which the temperature decreased from 1190 to 1100°C (shaded in Fig. 5) were less reliable due to uncertainties in discerning

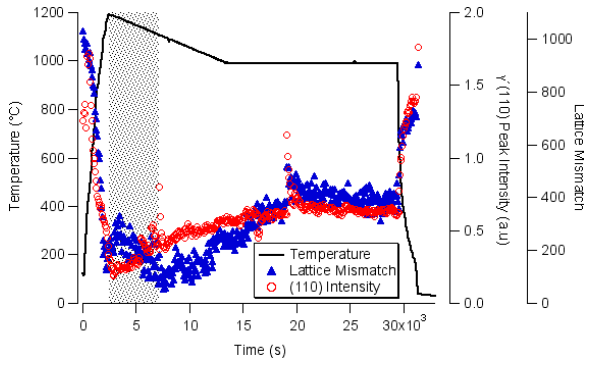

Fig. 5. Measured lattice mismatch between γ and γ′ phases, γ′ (110) peak intensity and temperature with time from as-received samples subjected to solutionizing, cooled to 1000°C, and held at that temperature for 5 h. The values of lattice mismatch in the shadowed area are not reliable due to the limitation of sensitivity of detecting small amounts of γ′ phase.

γ′ diffraction from background. However, below 1100°C the analysis showed the (110) peak intensity of γ′ phase gradually increased as the sample cooled to 1000°C. The intensity of the γ′ phase continued to increase over ~1.5 h after reaching 1000°C. Further aging at 1000°C did not result in any further changes in the intensity. The lattice mismatch between γ and γ′ phases was found to follow the peak intensity change. The lattice mismatch between γ and γ′ phase increased until it reached a maximum level. Interestingly, the overall change in the lattice mismatch in the second experiment was small compared with that of the previous experiment (see Figs. 4 and 5). The above results suggest that the γ′ phase precipitates near its equilibrium composition while cooling to 1000°C, beyond which there is no driving force for further diffusion and, as a result, no large changes in lattice mismatch.

Analysis of results from synchrotron diffraction experiments indicated some difficulties. Typical data obtained from the as-received sample subjected to experiment 2 is shown in Fig. 6.

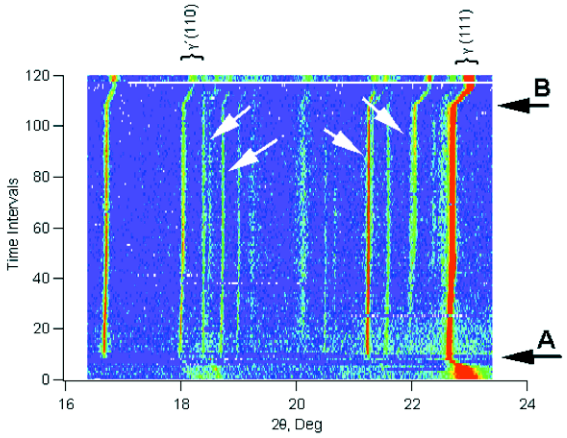

Fig. 6. Diffraction data obtained while subjecting the as-received sample to experiment 2 is shown in the image format (blue color corresponds to background and red color corresponds to maximum peak intensity). The data shows the period of γ′ dissolution and re-precipitation during heating (marked as A). The B arrow marks the completion of isothermal aging treatment at 1000°C. The white arrows indicate extraneous diffraction due to surface precipitation reactions.

The diffraction measurements successfully tracked the dissolution of γ′ phase during heating to high temperature. However, during re-precipitation of γ′ phase during cooling to 1000°C, in addition to (111) γ and (110) γ′ diffraction peaks, extraneous diffraction peaks from other surface precipitation reactions were observed. Surface precipitation reactions are unavoidable in nickel-base superalloys. In addition the diffraction quality was not sufficient enough to perform Rietveld refinement. Many combinations of refining angular and time resolution failed to improve the diffraction measurements. Therefore, the

results showed that the θ-2θ scanning diffraction instrument available at X14A beam line is not capable of performing time-resolved in situ diffraction experiments for nickel-base superalloys. In this regard, use of 2-D detector instruments with fast data collection may be a preferred choice. In addition, we need to devise methodologies to avoid extraneous diffraction from surface reactions.

Summary and Conclusions

We demonstrated for the first time that bulk microstructural changes in nickel-base superalloys could be characterized in situ using neutron diffraction with good time resolution. The results show that the microstructural evolution while aging at high temperature differs significantly depending upon the initial microstructure.

The benefits of the research are the following. First, the research demonstrated that it is indeed possible to track rapid microstructural changes with in situ neutron-diffraction technique using a high-flux spallation neutron source. The knowledge gained during this research will be useful in the design of engineering diffraction instrument for the Spallation Neutron Source (SNS). Second, the research showed that the lattice misfit between γ and γ′ phase in nickel-base superalloys could be controlled by obtaining a nonequilibrium microstructure coupled with post thermal treatments.

The results from this research were published in *Metallurgical and Materials Transactions*. In addition, the results were presented in an invited lecture during the High Temperature Materials Project 2001 symposium at the National Research Institute for Materials, Japan. Many researchers in the high-temperature materials project have shown keen interest in extending this work to understand other issues, including nucleation and growth. The results of the present research were also presented in a recent Joint Institute for Neutron Science meeting and lead to fruitful discussions with instrument scientists from other spallation neutron sources.

The concepts of this research were extended to research proposals submitted to the DOE. These proposals focused on extending the in situ phase transformation research in biomaterials, engineering alloys, and nanostructured materials.

References

[1]*Superalloys II*, ed. C. T. Sims, N. Stoloff, and W. C. Hagle, Wiley-Interscience, New York, 1987.
[2]H. Harada and H. Murakami, *Computational Materials Design*, ed. T. Saito, Springer, 1999, p. 39.
[3]C. Schmuck et al., *Phil. Mag. A.* **76**, 527 (1997).
[4]S. S. Babu et al., *Acta Materialia*, in press (2001).
[5]W. G. Williams et al., *Physica B*, **241–243**, 234 (1998).
[6]A. C. Larson and R. B. Von Dreele, *GSAS©–General Structure Analysis System*, LAUR 86-748, Los Alamos National Laboratory, 2000.
[7]T. Yokokawa et al., *Advances in X-ray Analysis*, **39**, 449 (1997).

Publications and Intellectual Property Derived from This Project

D. Q. Wang et al., "In-situ Characterization of γ/γ′ lattice stability in a nickel base superalloy by neutron diffraction," Metallurgical and Materials Transactions A **32A**, 1551 (2001).

S. S. Babu et al., "Nonequilibrium microstructure evolution in nickel base superalloys," submitted to *Materials Science and Engineering A*, in 2001.

Opportunities for Accelerator Mass Spectrometry at the Holifield Radioactive Ion Beam Facility

A. Galindo-Uribarri,[1] G. D. Alton,[1] R. Auble,[1] J. R. Beene,[1] J. Gomez del Campo,[1] B. Fuentes,[2] P. Hausladen,[2] R. C. Juras,[1] J. F. Liang,[2] M. Meigs,[1] D. C. Radford,[1] S. Raman,[1] and D. W. Stracener[1]

[1]*Physics Division*

[2]*The University of Tennessee*

The purpose of this project was to investigate the feasibility of using the highest-operating-voltage electrostatic accelerator in the world, the 25-MV tandem from the Holified Radioactive Ion Beam Facility (HRIBF), for accelerator mass spectrometry (AMS). A series of proof-of-principle tests indicate that it is possible to use HRIBF as a prototyping facility to aid in the development of new AMS methods. We focussed on areas where the high voltage of the tandem and the specialized instrumentation we have, or will develop, can play a unique role in AMS. We have special interest in the common technical challenges of both AMS and research with radioactive-ion beams (RIBs). We chose ^{36}Cl for the initial effort because it is an established AMS isotope with well-characterized samples available for analysis, and because the present sensitivity of measurements is limited by the ubiquitous presence of the stable ^{36}S isobar. In this report, we discuss our operational experience and development activities geared to optimize the implementation of an AMS system at HRIBF by systematically studying the factors that affect the sensitivity and accuracy of the technique.

Introduction

AMS is one of the analytical techniques with the highest sensitivity known in physics. It is used to perform ultra-sensitive measurements of concentration of rare isotopes in samples placed in the ion source of an accelerator system. This technique has important applications in environmental monitoring, in the study of ocean circulation patterns, radioactive waste, nuclear safeguards, and nuclear physics.

There are a number of similarities between AMS and RIBs. The removal of interfering isobars is one of the various common challenges of both AMS and RIB production. The physics associated with RIBs is currently one of the major thrusts of nuclear physics. The HRIBF is the first U.S. RIB facility devoted to low-energy nuclear structure and astrophysics research, making ORNL one of the leading laboratories in the RIB community. Strong support for a program of research at HRIBF to develop AMS techniques will benefit and be complementary to the production of RIBs. The DOE and NSF have just carried out a new Long Range Plan (LRP) exercise. The final report lists new opportunities in areas involving the construction of the Rare Isotope Accelerator (RIA) and its R&D program. For research at RIA to be viable, significant R&D is needed. This provides opportunities for developments in experimental methods, beam generation, and isobar separation. The LRP also stresses the importance of applications and interdisciplinary research of ongoing nuclear science activities.

The scope of this project was to investigate the feasibility of using the highest-operating-voltage electrostatic accelerator in the world, the 25-MV tandem from the HRIBF, for AMS. Initially our goal was to assess the potential use of the facility for the detection of isotopes such as ^{36}Cl, ^{44}Ti, ^{90}Sr, ^{99}Tc, ^{129}I, and ^{239}Pu. We choose ^{36}Cl for initial effort because it is an established AMS isotope with well-characterized samples available for analysis, and because the present sensitivity of measurements is limited by the ubiquitous presence of the stable ^{36}S isobar. The isotope ^{36}Cl, with a half-life of 301,000 years, has very important applications in AMS. For example, ^{36}Cl is a by-product of all reactor operations as it is produced by neutron activation of ^{35}Cl, which is present in trace quantities in all reactor materials.

Technical Approach

The research tasks included (1) developing beam diagnostic procedures for the low- and high-energy ends of the tandem, (2) establishing laboratory and sample preparation procedures, and (3) studying the stability and reliability of operation of the tandem. In particular, the ion source, beam optics, terminal voltage stabilization, and detection systems were carefully studied because they are extremely important in AMS. In the first stage of the project, we developed detection systems oriented to heavy isotopes. In the following we discuss the individual subsystems involved in the AMS proof-of-principle tests.

The ion source. Improvement of the overall intensity of the source will benefit the AMS program. We have available a single-cathode source which is adequate to get the AMS program started, but in the future we will require a new high-current multisample source designed to minimize "memory" effects due to sputtering from contaminated surfaces adjacent to the sample. We acquired the grid-point mesh program *NEDlab* to model the interior geometry of our Cs-sputter ion source with the aim of improving its performance, particularly concerning the negative ion output. Initial results indicate that modifications of the geometry could substantially improve the ion output. Source performance with new versions of the ionizer shroud, gas feed tube, and electrodes ultimately will test the success of the modeling of performance-enhancing modifications to the source. A systematic investigation of the negative ion current for various source-operating conditions was initiated. These conditions included increasing the amount of pumping in the source region, extraction optics, space-charge effects, and sample geometry.

Samples. The low background capabilities of AMS demand ultraclean sample preparation and specialized chemical processing techniques. For the tests with ^{36}Cl, we relied on samples in the form of silver chloride AgCl precipitated at IsoTrace Laboratory at the University of Toronto and pressed into a copper holder at HRIBF. Typical AMS sample preparation techniques for ^{36}Cl aim to reduce the stable isobar ^{36}S (0.02%), which can limit the count rate in the final detector. The background from the ubiquitous ^{36}S has plagued many AMS laboratories, forcing the use of complex detection schemes (e.g., gas-filled magnets) at AMS laboratories with smaller machines.

The injection system. Specialized injection systems for AMS have been developed in order to inject both the rare and abundant isotopes into the accelerator. AMS facilities that are shared with nuclear physics research such as the HRIBF 25-MV tandem, however, have not in general been modified for fast cycling. We are obliged instead to use slow switching and cycling. We explored changing the field in the mass-analyzing magnet. This is a comparatively slow process, with switching times of a few seconds. In principle, it is also possible to change isotopes by keeping all magnets fixed and changing only the preacceleration and terminal voltages. Although optics calculations showed negligible differences in the beam envelopes of the different isotopes, this process did not preserve isotope ratios to the high-energy end of the tandem. We still need to find a satisfactory method of quickly changing isotopes.

We began the implementation of instrumentation necessary for cycling of isotopes to measure the transmission of ^{35,37}Cl attenuated by a known amount. Because the ^{35}Cl/^{37}Cl ratio measured at the detector position is sensitive to drifts in beam tuning, it gives us a quantitative tool for measuring transmission and obviates the need to measure relative to a standard, although such samples are always necessary for the process of setting up.

The accelerator. HRIBF has a folded-geometry, 25-URC, tandem electrostatic accelerator manufactured by National Electrostatics Corporation. It has operated at terminal potentials up to 25.5 MV (highest in the world) with exceptional reliability. The desirable criteria for an AMS accelerator are that transmission of ions through the accelerator should be high and reproducible, that this transmission should be insensitive to small changes in the injection or accelerator parameters, and that the terminal voltage should be very stable. During the ^{36}Cl test runs, we used the signal from a generating voltmeter for beam stabilization. We were able to correlate and correct the data from unwanted ^{37}Cl due to recurrent voltage instabilities coming from two sections of the tubes. Shorting the tubes fixed the problem. We are considering a scheme with which we can continuously monitor and record the terminal voltage.

Post-acceleration analysis. Following acceleration, the charge state and hence energy of interest are selected using the tandem energy-analyzing magnet, which has a resolving power of up to 1 part in 12,000. Pure beams of light RIBs have been produced by fully stripping with a second carbon foil inserted on the beam path after the tandem.

Enge split-pole spectrograph. For the ^{36}Cl tests, we chose the use of the Enge split-pole spectrograph which provided further magnetic analysis needed to remove that small fraction of molecular fragments that acquired the correct energy to follow the same trajectory as the AMS isotope through the analyzing magnet. These fragments can otherwise cause unacceptably high counting rates in the ion detector. The AMS isotope continues to a final detector to further aid on the isobar separation.

Implementation of a dE-E telescope. A hybrid dE-E (gas/Si) detection system was implemented for the Enge spectrograph focal plane. A large-area solid state detector was installed as a residual energy detector inside an ionization chamber. Collection of the electrons produced in the active gas volume measure the energy lost by the ion along that portion of its track. Since ions of different Z lose energy at different rates, this energy-loss information permits the separation of isobars. A new Frisch grid consisting of a nickel mesh with 95% transmission and a 40-$\mu g/cm^2$ Formvar gas-confining window were installed. An ion chamber rotating support structure was built to allow alignment with the beam under vacuum.

Design and construction of a Bragg Curve detector. One promising direction is using an axial-field Bragg curve gas detector (BCD). In these detectors, the electric field is

parallel to the ion track and the energy-loss information is obtained from the time development of the signal at the anode. The designed BCD provides the versatility to double the detection depth with a second stage of electrodes within the same gas vessel to be able to stop the most energetic mid-mass ions required for the AMS program and for the *Z* identification of the RIB beam cocktails. The different components of the BCD were designed and acquired/machined to our specifications. The ultimate goal is to digitize the signal to optimize the *Z* identification capabilities of the detector even if the incident ions are not mono-energetic, such as the recoils from a nuclear reaction.

Time-of-flight systems. For heavier ions, the energy resolution of a gas or silicon detector is often insufficient to resolve neighboring masses. Better separation is possible by combining the energy measurement with a determination of the ions velocity via a time-of-flight (TOF) measurement. The ^{36}Cl tests did not require the use of TOF methods. We are considering the future use of TOF methods for AMS of fission fragments and for the first mass determination of some very neutron-rich RIBs.

X-ray detectors. It is possible to identify fast elemental ions by the characteristic X-rays they emit following excitation in a foil. We started a program to assess the projectile X-ray detection technique as a tool for isobar identification of heavier species of interest for both RIBs and AMS. A proposal was written and approved for beam time to study the X-ray yield dependence of energy, Z_{ion}, Z_{foil} for pairs of neighboring isobars. The technique was successfully used with neutron-rich RIB beams in recent experiments at HRIBF to monitor and determine the beam composition.

Fully stripped ions. The high energy and the equipment available at HRIBF enable the most sensitive measurements of ^{36}Cl by completely stripping all electrons with good efficiency. This guarantees a strong suppression of background events originating from the lighter isobar ^{36}S. This method can be extended to ^{14}C, ^{22}Na, ^{26}Al, ^{32}Si, ^{41}Ca, ^{44}Ti, ^{52}Mn, and possibly ^{60}Fe.

System performance. Studies related to the methodology of making measurements, such as charge-state distributions, transmission, and isotope switching were performed, while ion source cross talk and overall current were noted qualitatively. We engaged in systematically studying the factors that affect the sensitivity and accuracy of the technique.

Sensitivity. We elected to largely eliminate our ^{36}S background by fully stripping the ^{36}Cl to be measured, but the gain in cleanliness can only be realized as a gain in sensitivity if there is reasonable efficiency of conversion to this charge state. We measured the charge state distributions at the terminal (with both gas and carbon-foil strippers) and postacceleration (carbon-foil strippers) and determined that with the terminal voltages available at the HRIBF, we can produce the fully stripped charged state with an efficiency of roughly 8%. Combined with the high ionization efficiency of chlorine, we can in principle measure up to about 1% of the ^{36}Cl atoms present in a sample. (It is worth noting that to do this by decay counting would require 1% of a mean life, or about 4300 years.) In practice, the overall efficiency is lowered by transmission losses unrelated to charge state fraction. These losses are typically rather high, and only with exceptional effort are they as low as 50–60%. We undertook some systematic transmission studies because of the importance of eliminating these losses for both AMS and RIBs, but at present they are not understood.

Accuracy. The most difficult part of any AMS measurement is the interpretation of a number of counts in a detector as an isotope ratio. For the purposes of expediency, in the initial measurements, we measured the ratio of ^{36}Cl counts per time in a detector at the Enge focal plane to the periodically measured $^{35}Cl^-$ current at the low-energy Faraday cup for a standard of known ^{36}Cl/Cl ratio and assumed the same transmission for unknown samples.

Results and Accomplishments

The nuclide ^{36}Cl was chosen for initial effort because it is an established AMS isotope with well-characterized samples available for analysis, and because the sensitivity of measurements is limited by the ubiquitous presence of the ^{36}S isobar (the ^{36}Ar isobar is eliminated by use of a negative ion). We have concentrated on demonstrating excellent sensitivity while solving the technical problems necessary to make precise and repeatable measurements. In addition to measuring some previously characterized environmental chloride samples with ^{36}Cl/Cl ratios at the level of 10^{-14}, previously uncharacterized low-level reagent blanks and seawaters were measured in the range of 10^{-14} to 10^{-16} (Fig. 1).

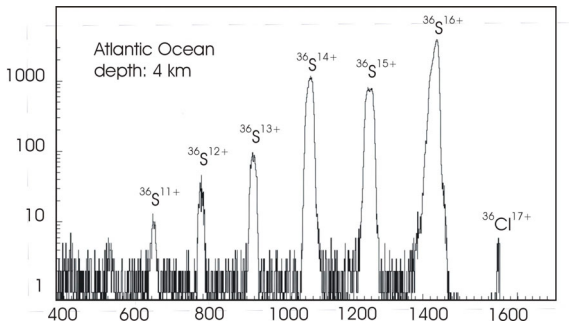

Fig. 1. Energy spectrum for A = 36 from a seawater sample. The peak corresponding to $^{36}Cl^{+17}$ is clearly separated from the $^{36}S^{+Q}$ "background."

Summary and Conclusions

A team of about a dozen individuals from the ORNL Physics Division complemented by outside collaborators from the University of Toronto explored the feasibility of an AMS program at HRIBF. The project allowed us to do some very successful proof-of-principle tests and to identify areas of strength at HRIBF aimed at establishing a research program for the development of experimental techniques for isobar separation useful for both AMS and RIBs. For the first time, an AMS experiment was performed at HRIBF to detect ^{36}Cl in a sea water sample. The results obtained proved that the HRIBF tandem is potentially the most powerful in the world for the measurement of ^{36}Cl.

This project has already promoted collaborative research with staff from the Chemical Sciences Division and external scientific groups. Recently, two of the codevelopers of AMS, H. Gove, University of Rochester, and A. E. Litherland, IsoTrace, University of Toronto, Canada, were at ORNL to discuss a joint effort for radiocarbon detection at the lowest possible levels. Among the possible applications discussed are the selection of low-concentration ^{14}C material for the detection of low-energy neutrinos and the radiocarbon dating of natural samples older than 60,000 years. Initial funding will be provided by NSF. Also, consideration is being given to a project involving the dating of Appalachian Rocks with the Geology Department of The University of Tennessee. Future collaborations are expected with other institutions that have expressed interest in our AMS results including Lawrence Livermore National Laboratory, Bedford Oceanographic Center, The University of Tennessee, and Instituto Nacional de Investigaciones Nucleares. A description of our operational experience and development activities of the AMS program at HRIBF was given in various talks.

Mass Measurements of Short-Lived Nuclei at the Holifield Radioactive Ion Beam Facility

D. C. Radford,[1] C. Baktash,[1] J. R. Beene,[1] A. Casares,[2] R. Hatarik,[3] and H. Wollnik[2]
[1]*Physics Division*
[2]*Department of Physics and Astronomy, The University of Tennessee*
[3]*Justus-Liebig University Giessen, Giessen, Germany*

The purpose of this project was to determine the feasibility of a high-precision time-of-flight mass analyzer. This device will be used for a new program of mass measurements of short-lived radioactive ions at the Holifield Radioactive Ion Beam Facility. Such measurements provide information crucial to both nuclear structure physics and nuclear astrophysics. The device is remarkably compact yet should be capable of a mass precision of about 1 ppm after a flight time of approximately 1 ms. We have assembled a proof-of-principle prototype of such a device and achieved a mass resolution (FWHM) $\Delta m/m$ of approximately 1/20,000. With a larger improved device, and better high-voltage power supplies, we hope to obtain $\Delta m/m$ close to 10^{-5}, which should allow the desired precision of 1 ppm. A decision will be made early in CY 2002 on submitting a proposal to DOE for construction of an operational device.

Introduction

Experiments with radioactive ion beams offer exciting research opportunities in nuclear structure physics and in nuclear astrophysics. Such research can be carried out at the Holifield Radioactive Ion Beam Facility (HRIBF) at ORNL, which is currently the only on-line isotope-separator facility in the United States that can produce and post-accelerate ions of short-lived nuclei.

We believe it would be highly desirable to institute a program of precision mass measurements of short-lived isotopes at the HRIBF. This most fundamental of nuclear properties can provide information crucial to both nuclear structure physics and nuclear astrophysics. The precision desired for new mass measurements is about 100 keV or better, which corresponds to approximately 1 ppm for nuclei of mass around 100. Moreover, in order for such measurements to be applicable to short-lived nuclei, one must be able to perform them within a time that is less than or comparable with the nuclear lifetime. For species with previously unmeasured masses, this generally means lifetimes significantly less than 1 s.

There are, at present, no facilities at the HRIBF suitable for precision mass measurements. The present proposal had the goal of laying the groundwork for mass measurements by developing a proof-of-principle prototype of a new multi-pass time-of-flight mass analyzer (MTOF-MA). Such a device would be both less expensive and more versatile than the well-known Penning trap mass spectrometers or large storage rings that are now used for this purpose. An MTOF-MA can determine an ion mass with uncertainties of less than 1 ppm in less than 1 ms and is therefore ideally suited to the investigation of unstable neutron-rich nuclei with lifetimes of 1 ms or longer and also can be applied to a large percentage of the neutron-deficient nuclei.

Technical Approach

The basic operating concept of an MTOF-MA is straightforward. In the form which would be implemented at a radioactive ion beam facility, the ions whose masses are to be measured are first decelerated to energies of ~100 eV, then introduced into a gas-filled RF-quadrupole where they are cooled to thermal energies. After cooling, the ions are re-accelerated to energies of a few kiloelectron volts and simultaneously bunched to a few nanoseconds, before being injected into the MTOF-MA, where they travel repeatedly along a linear flight path between two electrostatic ion mirrors. They may undergo as many as several hundred reflections between these mirrors before being released for detection. The ion mass is then determined from a precise measurement of the total flight time.

Mass analyzers of the MTOF-MA type have not yet been employed in nuclear physics research; however, elements of the system we plan to develop have been built. An MTOF-MA without the RF-quadrupole cooling stage has been built and tested for applications on space missions.[1,2] In a separate development, a gas-filled RF-quadrupole that can cool 100-eV ions has also been successfully demonstrated at several laboratories; see, for example, Ref. 3.

The basic goal of our proposal was to assemble and test a small prototype MTOF-MA. We concentrated on assembly and testing of the critical mirror and time-of-

flight components, which form the heart of the MTOF-MA, and on determining what mass resolving power can be achieved. For simplicity and economy, these measurements were made with stable ions, formed in an electron-impact bunching ion source. However, since the main goal of our effort is the study of short-lived species, we also required that the mass measurement be performed in an elapsed time of within 1 ms.

Results and Accomplishments

A small prototype MTOF-MA developed for Ref. 1 was obtained and adapted as a proof-of-principle device for the present project. This device has a total length of less than 1 m; the two electrostatic mirrors are about 30 cm apart. A turbo-molecular pumping system was purchased, as were some high-precision, high-stability high-voltage (HV) power supplies, a multi-channel delay generator, and microchannel plates (MCPs) to serve as an ion detector, etc.

A data acquisition system consisting of a PC with a control card and a high-precision time-to-digital converter (TDC) was assembled. A control system for the fast switching of the HV for the ion source and electrostatic mirrors, and triggering of the data system, was implemented. Software for the acquisition, display, and analysis of time-of-flight spectra was developed; spectra from this software can be seen in Figs. 1 and 2.

A small electron-impact bunching ion source and the MCP detector were installed, and the full system then tested and tuned. Mass spectra were obtained for natural krypton and also for a mixture of nitrogen (N_2) and carbon monoxide (CO) gases. The former, in Fig. 1, shows mass peaks at the naturally occurring krypton isotopes A = 80, 82, 83, 84 and 86. The latter is displayed in Fig. 2, and has two A = 28 peaks, separated by 0.011 mass units (10.5 MeV) or one part in 2,500. From these measurements, it was determined that a mass resolving power of at least

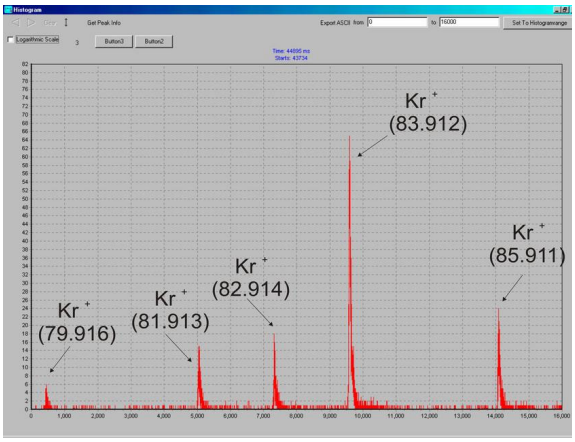

Fig. 1. Time-of-flight mass spectrum for krypton ions, showing five naturally occurring isotopes with the labeled masses.

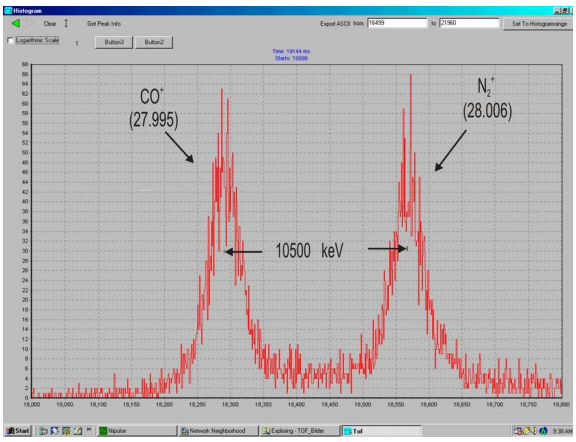

Fig. 2. Time-of-flight mass spectrum for a mixture of N_2 and CO ions, showing the two mass peaks with a separation of 0.011 mass units.

Δm/m ~1/20,000 (FWHM) is achievable with this prototype MTOF-MA, as presently configured, using a flight time of under 1 ms. While this is an extremely encouraging result and indicates that even this prototype device could provide meaningful measurements, we anticipate that it should be possible to substantially improve the resolving power, perhaps by as much as a factor of five.

It was determined that, as expected, the quality of the HV power supplies used in the electrostatic mirrors and lenses is crucial for obtaining good mass resolution. Ripple and drift on the supplied HV modify the ion trajectories and their flight time and thus degrade the performance of the system. We believe that this effect is one of the dominant limitations of the current device and we plan to replace some of the lower-quality HV supplies that we have been using with new, better ones. We also believe that we can obtain further gains in mass resolving power by increasing the size of the MTOF-MA and applying some minor modifications to the geometry of the electrodes that comprise the electrostatic mirrors. To this end, we performed calculations of the electric field distributions and simulations of ion trajectories, for various trial electrode geometries. One such calculation is shown in Fig. 3.

Before the mirror time-of-flight system discussed above can be used to make mass measurements of short-lived species at a radioactive ion beam facility, it must be matched and incorporated with an appropriate beam cooling system. An electrostatic decelerator, gas-filled RF quadrupole beam cooler, and re-accelerator system for negative ions[3] has recently been tested at the HRIBF. This system, with some minor improvements, would be quite suitable for the purposes of this mass analyzer. However, an ion buncher will need to be designed and added to the beam cooler in order to prepare the ions for injection into the final MTOF-MA.

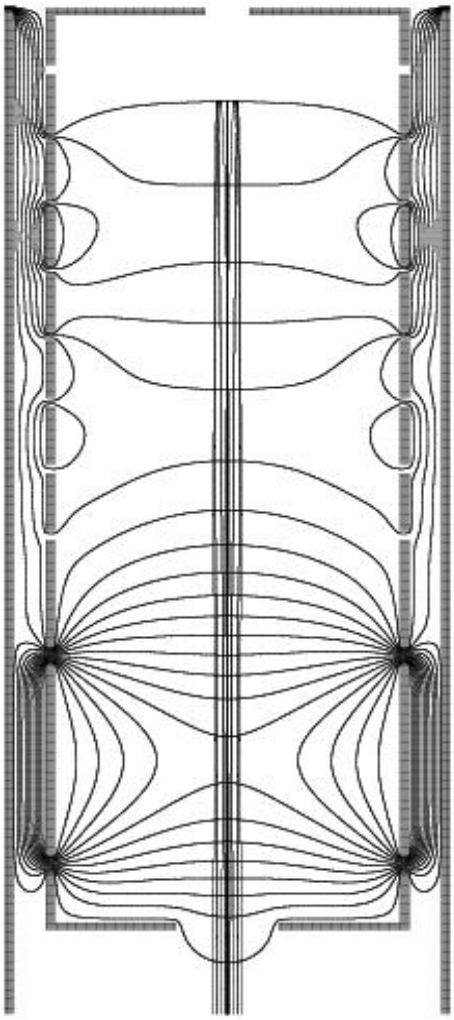

Fig. 3. SIMION calculation for one candidate geometry of an upgraded mirror electrode system.

Summary and Conclusions

The feasibility study of a high-precision time-of-flight mass analyzer for a new program of mass measurements at the HRIBF proceeded well. We assembled a proof-of-principle prototype, together with associated electronics and data acquisition system, and demonstrated that it is capable of a mass resolving power (FWHM) $\Delta m/m$ of approximately 1/20,000. With a larger improved device, and better HV power supplies, it should be possible to obtain $\Delta m/m$ close to 10^{-5}, which would allow the desired precision of 1 ppm. In CY 2002, a decision will be made on submitting a proposal to DOE for construction of an operational device.

Assuming that we are successful in obtaining funding from the DOE Nuclear Physics Program Office to build a full-scale, operational device, we will then incorporate it into our experimental program. In addition, the expertise and experience demonstrated in this project has made ORNL a prime candidate to develop similar mass analyzers for the advanced radioactive beam facility, Rare Isotope Accelerator, now being planned by DOE to be operational in about ten years time.

The MTOF-MA system we envisage has great potential for the study of radioactive nuclei and is more flexible than existing mass analyzers. This is not only because it can be used to measure the masses of much shorter-lived species but also because it is a comparatively compact and open structure that will allow a variety of decay measurements to be made along with the basic mass measurement. We expect this to lead to the development of several powerful new experimental techniques.

References

[1]A. Casares, A. Kholomeev, N. Nankov, R. Roll, H. Rosenbauer, and H. Wollnik, 47th American Soc. for Mass Spect. Abstracts, abstract 084 (1999).

[2]A. Casares, A. Kholomeev and H. Wollnik, Int. Jou. Mass Spect. **206**, 267(2001).

[3]Y. Liu, J. F. Liang, G. D. Alton, J. R. Beene, Z. Zhou, and H. Wollnik, *Nucl. Instr. Meth. B*, in press.

Publication Derived from This Project

H. Wollnik and A. Casares, Federation of Analytical Chemistry and Spectroscopy Societies Conference, Detroit, October 2001, abstract 356, p.182.

Solid Hydrogen Target for Radioactive Beam Experiments

D. Shapira,[1] M. J. Saltmarsh,[2] J. R. Beene,[1] T. A. Lewis,[3] L. R. Baylor,[4]
S. K. Combs,[4] and D. A. Rasmussen[4]
[1]*Physics Division*
[2]*Joint Institute for Heavy Ion Research*
[3]*Engineering Science and Technology Division*
[4]*Fusion Energy Division*

We have tested the feasibility of applying solid hydrogen extrusion techniques, developed at the Fusion Energy Division at ORNL, toward the production of targets of solid hydrogen to be used in nuclear physics experiments. A new nozzle, through which a flat sheet of hydrogen can be extruded, was designed, built, and tested. Solid hydrogen sheets were successfully extruded. Visual inspection indicated that they were without major flaws, and stable over time. In two following experiments, quantitative measurements of target thickness and uniformity were performed with a radioactive source of energetic α particles and a solid-state detector set up in positions facing each other and straddling the target region. For these two experiments, target lifetimes were more than adequate, but target uniformity was poor. This was apparent both from visual inspection and the α source measurement. Improving the uniformity and reliability will probably require separate temperature control of the extruder and target regions.

Introduction

The advent of radioactive ion beam (RIB) facilities, such as the Holifield Radioactive Ion Beam Facility (HRIBF) at ORNL, provides us with exciting new opportunities to study nuclear reaction and nuclear structure in regions farther away from the valley of stability. These opportunities have been summarized in the 1997 report to the Nuclear Science Advisory Committee[1] and include reactions of interest to both the nuclear physics and astrophysics communities.

Most of our early knowledge in nuclear science came from studies of reactions induced by hydrogen and deuterium nuclei on targets containing stable nuclei. However, stable nuclei cover only a small fraction of the region of interest. The availability of radioactive nuclear beams coupled with hydrogen targets can extend the reach of similar studies many-fold. An ideal target would be clean (single isotope), uniform, and of compact dimensions. A sheet of hydrogen ice is as close as one can get, provided it can be produced reliably with variable thickness, a high degree of uniformity, and could last long enough for nuclear reaction studies to be performed on it. Such a target would be of great value to the nuclear physics and astrophysics communities. Of particular interest to HRIBF users is a range of target thickness below 10 mg/cm^2.

Solid hydrogen targets in this thickness range are difficult to maintain, as evaporation rates at temperatures $\gtrsim$5 K result in significant loss of thickness in times $\lesssim$1 h. However, application of the hydrogen extrusion techniques developed for fusion fueling systems would allow the target to be continuously renewed, off-setting the losses due to evaporation.

Technical Approach

The objective of this work was to demonstrate that hydrogen extrusion techniques could be applied to the formation of a thin (~2 mg/cm^2) target suitable for nuclear physics studies. The critical issues to be addressed were the following:

(a) The controlled formation of a relatively thin sheet of solid hydrogen.
(b) Thickness and uniformity of the solid hydrogen target produced in this way.
(c) Variation of target thickness over time (due to evaporation and deposition on the surface).

Hydrogen Extrusion

For this experiment, an existing hydrogen extruder system in the Fusion Energy Division was used to supply solid hydrogen ice. The system includes the mechanical hardware and instrumentation, controls, as well as the vacuum and gas systems required for making and maintaining hydrogen ice. The extruder design is based on that originally developed by Foster[2] for feeding hydrogen ice to centrifuge injectors for plasma fueling of fusion plasmas. Similar extruders have been used in pneumatic pellet injection systems for plasma fueling,[2–7]

and the extruder system used here is a development device of this class. The apparatus shown in Fig. 1 serves both to solidify (or freeze) hydrogen isotopes and to force-feed the resulting ice to a transition section. A motor-driven screw press (not shown) actuates a piston running in a brass sleeve (inside diameter = 1 cm), which is brazed at both ends to oxygen-free (OFHC) copper blocks. These blocks are convectively force cooled by helium (liquid and/or gas) flowing through cooling channels on their exteriors. The top block or liquefier is controlled near the triple-point temperature of the gas, which is below the saturation temperature of the gas feed but above the melting point of the solid. The lower block or freezer cylinder fills automatically as the gas condenses on the sub-cooled walls of the liquefier. When the piston is fully retracted, the condensate drains through channels machined in the top of the brass sleeve and fills the cylindrical cavity in the second heat exchanger. The liquid eventually (within a few minutes) freezes in this region, which is maintained at several degrees below the gas triple-point temperature. Upon freezing of a charge (typically 4 cm^3 of ice), the extruder is ready to supply solid material to the acceleration section of the injector. The piston speed (and thus the extrusion time) is controlled by an electronic motor control package. A transition nozzle mounted on the bottom of the freezer determines the final size of the ice ribbon. In our case, a ribbon of ice with cross-sectional area of 10 mm × 0.3 mm is formed. A circular opening is allowed for ion beams to enter the designated target area and for nuclear reaction products to exit. Maximum extrusion forces can vary from a few hundred to thousands of pounds, depending on the extrusion temperature, transition nozzle geometry, and extrusion rate. A force washer is used to monitor the extrusion force, and an adjustable electronic interlock is available to limit the extrusion force to safe operating levels (typically 1000 lb f for standard design).

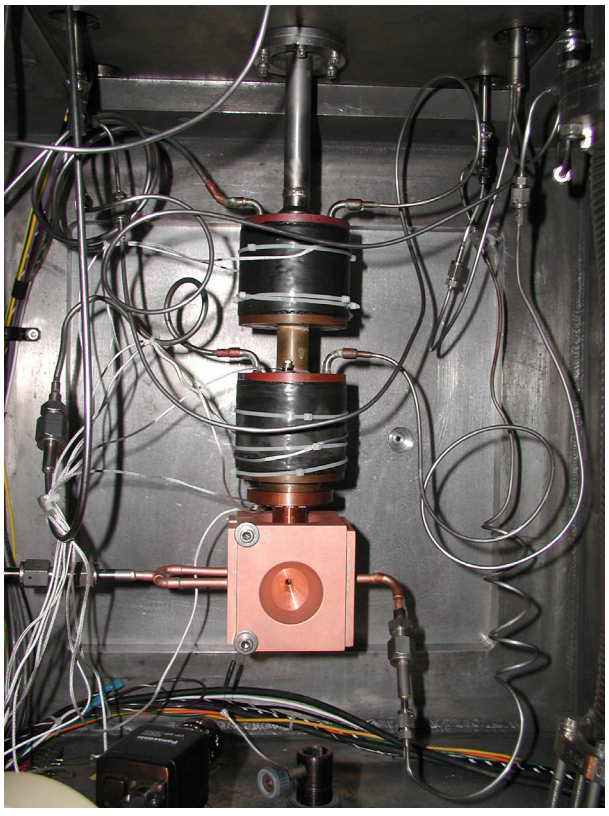

Fig 1. Photograph of the extrusion apparatus. The copper block at the bottom is the target region where the hydrogen ribbon can be viewed through the beam access hole.

Studying energy loss by charged energetic ions in the target material allows for quantitative evaluation of target thickness and uniformity. A 10-mCi radioactive ^{229}Th source deposited[7] on a small glass disk emits α particles, and their energy spectrum is measured in a silicon surface-barrier detector. The source and detector straddle the target location, and a comparison of the spectra of α particles that reach the detector with and without the hydrogen target in place yields information on the hydrogen target thickness and uniformity.

Figure 2 shows a schematic depiction of the experimental setup used in the experiment. Figure 3 show results of a test run where a particles reaching the detector were recorded with and without an intermediate 25-μm-thick aluminum foil inserted between the detector and the α source. The shift in energy provides a measure of foil thickness, and the increase in width (worse energy resolution) results from the combined effect of energy straggling in the foil and foil in-homogeneity.

Results and Accomplishments

Extrusion of Thin Sheets

Initial attempts to extrude the 10 mm × 0.3 mm hydrogen sheets were successful, although the operating envelope of extrusion force and extrusion temperature was very restricted. Figure 4 is a picture of the target region showing a thin (300-micron) sheet of frozen hydrogen

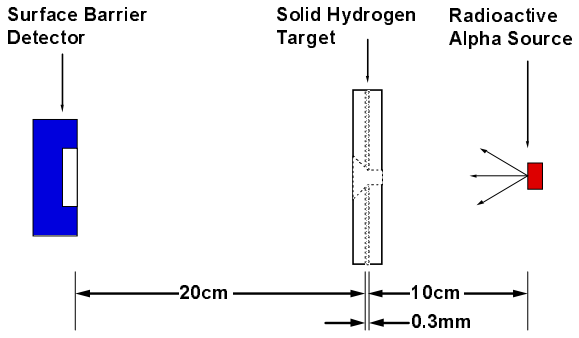

Fig. 2. Setup used for target thickness measurements.

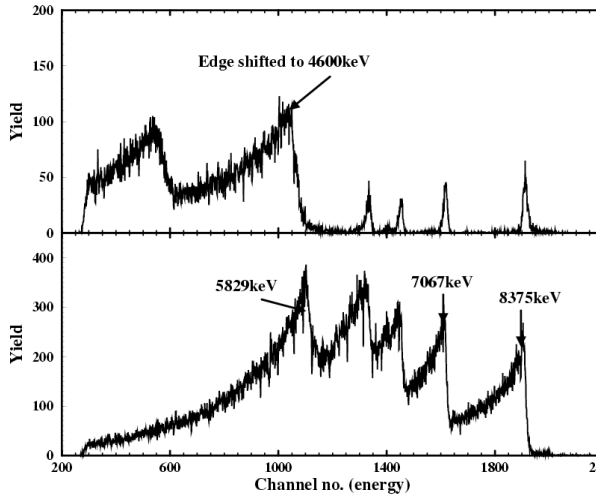

Fig. 3. Energy spectrum of α source. Upper part shows the shifted spectrum. The smaller peaks at high energy represent leakage through holes in the thin aluminum foil.

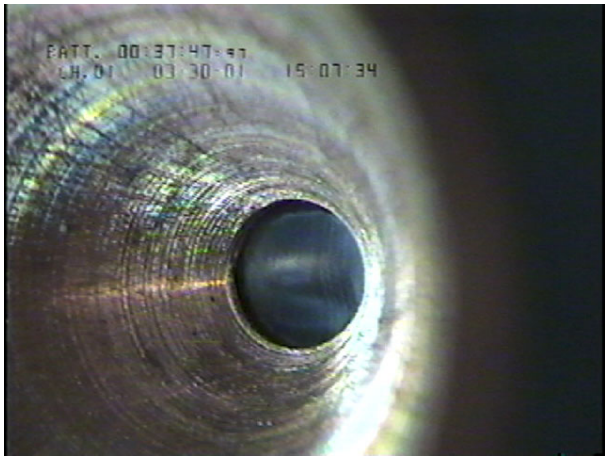

Fig. 4. Photograph of the hydrogen target taken through the 5-mm access hole in the copper block. The extrusion was stopped when the picture was taken.

completely covering the 3-mm-diameter target region. Visual inspection of this picture, and the 10-min video from which it was taken, show no gross imperfections or non-uniformities during the extrusion process. The extrusion temperature was 6.7 K, and the force required was somewhat greater than the 1000-lb f limit of the instrumentation used.

The picture was taken during a period when the extrusion was stopped and the temperature of the extruder and the target region was allowed to drop to about 5 K. The solid hydrogen was left for 6 min, during which time no visible changes occurred to the hydrogen sheet.

In two later experiments with added diagnostic capability, the operational parameters for the extrusion process were established. These are listed in Table 1, together with the data from the initial experiment.

Table 1

Extrusion temperature (K)	Extrusion force (lb f)	Extrusion rate (mm/s)
6.7	>1000	?
6.85	1340	0.11
7–7.1	1420	0.08

As previously mentioned, the operating temperature envelope proved to be very restricted. At slightly lower temperatures, the extrusion force required exceeded the limits of the existing apparatus, while at higher temperatures there was an added risk of runaway evaporation in the target region. Introducing separate temperature controls for the extrusion nozzle and target regions would relieve these restrictions by allowing the target region to be held at 4.2 K while the extrusion temperature was raised to lower the yield stress of the hydrogen.

In the two later experiments, the visual quality of the hydrogen sheet was not as good, as shown in Fig. 4. Large defects, including holes, could often be seen. The narrow operating window may have contributed to this problem, although the possibility of dirt, and imperfections, or misalignment in the extruder assembly cannot be ruled out.

The extrusion rates observed, while acceptable, were somewhat higher than those necessary for the target application (~.01 mm/s). Again, separate temperature control of the target region would make it easier to lower the extrusion rate and extend the estimated time between fills of the hydrogen reservoir from hours to days.

Target Uniformity

The required uniformity in target thickness was ~10%. The two later experiments for which the α source measurements were available were also those for which the uniformity was visibly poor. From measurements of the α-energy spectrum after transmission through the target, we inferred a large variation of thickness across the target, as might be expected when holes were visible. This is shown in Figs. 5a–5c, where the spectrum observed with no hydrogen is compared with that observed with hydrogen at three different times. Deconvoluting the thickness profile from such data cannot be expected to provide detailed information of the profile but can be used to estimate the gross features. The lines through the data represent fits obtained by manually adjusting the assumed thickness profiles, and degrading the initial a spectrum in energy by taking an average value of the stopping power for as in hydrogen in the relevant energy range of 4 to 8.4 MeV. This method, while not ideal, was sufficient to

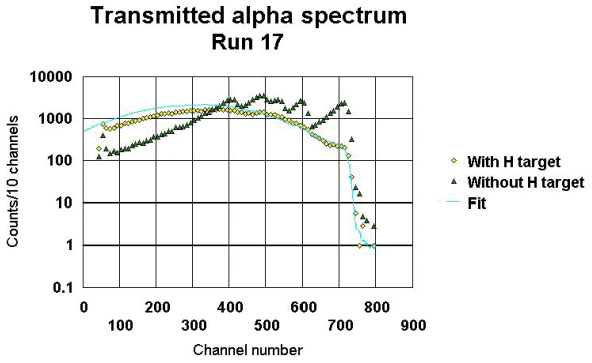

Fig. 5a

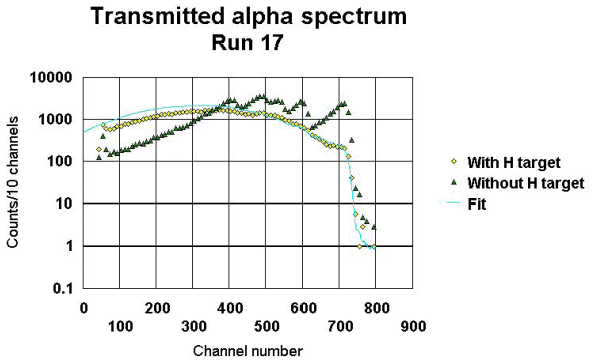

Fig. 5b

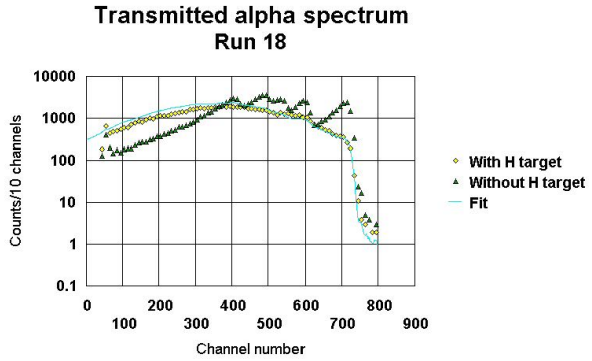

Fig. 5c

Fig. 5. Energy spectra of α-particles reaching the detector through the hydrogen ice sheet being in place for (a) 2.4 min, (b) 10.5 min, and (c) 15.5 min.

show that the variations in thickness were indeed large, consistent with ±100% of the average thickness in each case.

Target Lifetime

From data shown in Fig. 4, average thicknesses of the hydrogen sheet at the three different times were estimated, and the results are given in Table 2.

Table 2

Run ID	Time after formation (min)	Average thickness (mg/cm^2)	Variation in thickness
16	2.5	1.23	~±100%
17	10.5	1.01	~±100%
18	15.5	0.76	~±100%

The data in Table 2 were taken after the extrusion had been halted. The temperature of the extruder and target region was lowered from the extrusion temperature of 7 K down to the temperature of the liquid helium coolant, 4.2 K. From these results the estimated evaporation rate of the target is approximately 40 mg/cm^2/min. This is satisfyingly close to the rate of 70 mg/cm^2 estimated assuming the surface temperature to be 5 K with no allowance for evaporative cooling. For a 2-mg/cm^2 target this would imply that 10% of the target would evaporate in about 5 min, which in turn would require a moderate extrusion rate >0.02 mm/s to keep thickness variations below the 10% goal.

Summary and Conclusions

The project goal was to demonstrate that the technique of hydrogen extrusion could be used to form relatively thin sheets of solid hydrogen suitable for use as targets for nuclear and astrophysics studies. The three key technical objectives were as follows:

(1) To show that thin (~300 μm) hydrogen sheets could be extruded. This was done successfully, although good quality films could not be formed reliably.

(2) To establish that a target uniformity of about 10% could be achieved. This was not done. The measured uniformity was very poor. However there was evidence from our initial runs—when the thickness diagnostic was not in place—that much better results were possible.

(3) To establish that appropriate combinations of evaporation rate and extrusion rates could be attained to reach target lifetimes of hours–days. The results obtained support this conclusion and were somewhat more favorable than our original estimates.

Further R&D will be needed to improve the reliability and uniformity of the system. Separate temperature control of the extrusion and target region will be required to expand the operational window and can be expected to improve reliability. In addition to this, further work on the effect of surface treatment, surface cleanliness, and alignment techniques for coupling the different extruder parts are needed to improve the uniformity.

The concept was presented at the RIA2000 workshop last year and at a seminar at Michigan State University. In addition, brief reports of the early results have been given at two recent DOE-sponsored reviews of the HRIBF

nuclear physics program and at the Fourth Latin American Workshop on Nuclear Physics. These have established ORNL's credentials in the development of solid hydrogen targets and in the use of fusion extrusion technology for this application.

Two routes for follow-on funding will be pursued. Once the ongoing Nuclear Science Advisory Committee review of nuclear physics programs is complete, and assuming that the review of the ORNL RIB program is positive, we shall propose an R&D effort to DOE's Division of Nuclear Physics aimed at near-term applications at the HRIBF. This will prepare the way for a later proposal to the Radioactive Ion Beam facility R&D program, for which thicker targets will be required.

References

[1]J. D. Garrett et al., "Plans for Constructing Next-Generation ISOL Facility at ORNL," *AIP Conference Proceedings* **473**(1), 466–476 (April 1999).

[2]C. A. Foster, "Solid Deuterium Centrifuge Pellet Injector," *J. Vac. Sci. Technol.* **A1**, 952 (1983).

[3]S. K. Combs et al., "Repeating Pneumatic Hydrogen Pellet Injector for Plasma Fueling," *Rev. Sci. Instrum.* **56**, 1173 (1985).

[4]S. K. Combs et al., "Operation of Repeating Pneumatic Hydrogen Pellet Injector on TFTR," *J. Vac. Sci. Technol.* **A4**(3), 1113 (1986).

[5]S. K. Combs et al., "Eight-Shot Pneumatic Pellet Injection System for the Tokamak Fusion Test Reactor," *Rev. Sci. Instrum*. **58**, 1195 (1987).

[6]S. K. Combs et al., "New Extruder-Based Deuterium Feed System for Centrifuge Pellet Injection," *Rev. Sci. Instrum.* **68**, 448 (1997).

[7]S. Mirzadeh, Nuclear Science and Technology Division, ORNL, personal communication with M. Saltmarsh, Joint Institute for Heavy Ion Research, November–December 2000.

Collisional Transport of Charged Particles and Energy in Complex Magnetic Fields

S. P. Hirshman,[1] E. F. D'Azevedo,[2] L. A. Berry,[1] D. A. Spong,[1] B. Peyton,[2] and W. F. Lawkins[2,3]
[1]*Fusion Energy Division*
[2]*Computer Science and Mathematics Division*
[3]*Mathematics Department, The University of Tennessee*

The purpose of this project was to enhance ORNL's capabilities for computing transport coefficients in complex, three-dimensional (3-D) magnetic fields arising in low-aspect-ratio stellarators. Toward this end we performed theoretical analysis of the structure of the underlying block-tridiagonal system of linear equations describing transport in such devices. This investigation was restricted to the 3-D phase subspace comprised of two spatial angular coordinates and one velocity pitch-angle coordinate, with the intent that the iterative methods investigated will eventually be extensible to higher spatial and/or velocity dimensions. The original code for solving this subspace problem, which was based on the block Thomas algorithm and is therefore *not* extensible to higher dimensions, was nevertheless successfully reformulated in terms of Kronecker products to provide convergent solutions at low collisionalities (a regime of physical importance where it had previously failed to converge). Several extensible iterative procedures using preconditioners based on these Kronecker products were investigated. This work has positioned ORNL to compete for major funding in the Plasma Science Advanced Computing Initiative (PSACI), an element of the newly approved Scientific Discovery through Advanced Computation initiative (SciDAC), and to play a leading role in extracting physics results from the $1 billon-class stellarator experiments coming on line.

Introduction

Stellarators are toroidal devices that confine hot plasmas—using complex magnetic fields produced largely by external coils—long enough so they can undergo substantial controlled thermonuclear reactions before scattering out of the device. There is considerable interest in stellarators worldwide, with several $1 billion-class machines on line now or expected in the next few years. In the United States, the design of low-aspect-ratio stellarators has been the focus of much theoretical effort aimed at building at least two such devices in the next few years. One is envisioned at ORNL, the so-called Quasi-Poloidal Stellarator (QPS). These activities have reinvigorated the U.S. stellarator community and laid the groundwork for an exciting experimental program within the Fusion Energy Division at ORNL.

While the stellarator has advantages compared to the axisymmetric tokamak (a stellarator is easier to operate in steady state and is resilient to current-driven instabilities), a potential disadvantage is the increased plasma particle and energy losses due to reduced symmetry resulting from the 3-D magnetic fields. Understanding these losses is a critical issue for stellarator development, and is a major objective of the world fusion experimental programs. We are developing codes to analyze the transport of electrons and plasma ions in such devices, where the high-temperature regime of interest means that collisional scattering is very infrequent and complex particle drifts and trapping effects dominate the orbit topology. This situation leads to an equation for the particle distribution functions that exhibits local boundary layers in phase space ("shocks") that are determined by the subdominant collisional processes. We have investigated several iterative techniques, which are needed to extend the solution capabilities to higher dimensions (both in real and velocity space). For these methods to be efficient, it is necessary to find suitable preconditioning algorithms applicable to this problem characterized by large condition numbers. Kronecker-product forms have been developed to concisely factor the large multidimensional matrices arising in the preconditioner.

Technical Approach

The fundamental equation describing the transport processes in a high-temperature stellarator is the drift-kinetic equation for the time evolution of the plasma distribution function $f(x,v)$ resulting from particle motion (which include streaming *along* magnetic field lines and drifts *across* the magnetic lines) and small-angle scattering processes (collisions). The new stellarator experiments and reactors will operate in very high-temperature regimes where collisions are infrequent and particle orbits are strongly affected by the 3-D stellarator magnetic field (the neoclassical "1/ν" regime). In this regime, particles can be

trapped in local magnetic wells for part of their orbit as they continually drift across magnetic flux surfaces, introducing new physics. To address this physics accurately, the dimensionality of the computational problem must be increased from the present three dimensions (two real space, one velocity space, coordinate) to four dimension (three real space, one velocity space). In addition, energy diffusion, important for the radio frequency (RF) heating that is needed to heat and control the stellarator plasma, introduces yet another dimension.

To position ORNL for research programs based on developing this higher dimensionality physics, advances in the physics and numerical approach to the 3-D problem are needed. Thus, while our theory efforts have been applied to the simpler 3-D problem, it is intended that the techniques developed here will be eventually extensible to problems of interest in higher dimensions.

In the past, pioneering research[1] at ORNL led to the development of the 3-D drift-kinetic equation solver (DKES code). Solutions of the drift-kinetic equation are presently obtained by DKES using a block variant of the Thomas algorithm for LU factorization of a tridiagonal matrix. Spatially averaged velocity moments of the distribution function obtained from DKES are used to compute transport coefficients from which macroscopic transport rates are estimated. Due to the sequential nature of this algorithm, there is only limited opportunity for parallel computation within the dense blocks. Orthogonal Legendre polynomials for the velocity pitch-angle variable dependence are used to generate the sparse block tridiagonal structure. The block size is determined by the number of spatial Fourier modes (sine and cosine), and the overall number of blocks is determined by the degree of Legendre polynomials. While the original code is efficient for small problems, there is concern about conditioning for larger systems. A scalable algorithm is also needed to efficiently exploit the current generation of supercomputers. Therefore we have considered a preconditioned iterative method.

The success of an iterative method depends on an efficient preconditioner and an efficient method for computing matrix-vector products. By taking advantage of the variable separation structure of this matrix problem, the linear system can be decomposed as a sum of four matrices, each of which can be represented by a Kronecker product of two smaller matrices.[2] The four Kronecker products correspond to the different physical components of the differential operators in the drift kinetic equation. The Kronecker product has many features that make it well suited for parallelization. If matrix A is n by n and B is m by m, then the Kronecker product matrix C = $A \otimes B$ is mn by mn. Moreover, $C^{-1} = A^{-1} \otimes B^{-1}$, $C^T = A^T \otimes B^T$, and matrix multiplication can be computed very efficiently as $Y = CX = (A \otimes B)\, X = (B\, X)\, A^T$. This requires only O[$nm(n+m)$] operations, which is much smaller than the O[$(mn)^2$] operations nominally required without this factorization.

We have conducted numerical investigations and experiments with MATLAB using the memory efficient representation afforded by these Kronecker products. We have found that in the very low collision frequency regime under investigation, the linear systems contain eigenvalues with dominant imaginary components. This type of eigen-spectrum poses a severe challenge to the standard iterative Krylov methods such as BICGSTAB, GMRES, or QMR.

The DKES matrix can be written as

$$C = \Sigma\, A_I \otimes B_I \ ,$$

where I=1,…,4 and the tridiagonal matrices A_I arise from the Legendre orthogonal polynomial representation and dense matrices B_I arise from spatial Fourier modes. Some of these matrices are also rank deficient, which further complicates the preconditioning analysis. The preconditioning step can be considered as an operation that takes a residual vector as input to produce an approximate solution. We have considered several preconditioners:

1. Inverse of dominant Kronecker product. Given a residual vector r, we return $x = (A_1 \otimes B_1)^{-1} \times r$ or $x = (A_1^{-1} \otimes B_1^{-1}) \times r$ that can be implemented as $x = B_1^{-1} \times r \times (A_1^T)^{-1}$.
2. Inverse of the two most dominant Kronecker products: $[\,(A_1 \otimes B_1) + (A_2 \otimes B_2)]^{-1}$. The inverse can be computed via a generalized eigen-decomposition of B_1 and B_2. The decomposition can be computed once and reapplied for each preconditioning step.
3. This precondition is similar to the above of using sum of two Kronecker products that are closest (in Frobenius norm) to matrix C. The Nearest Kronecker Product (NKP) problem can be approximated by finding the dominant two singular values and vectors using an iterative method.[3] The full singular value decomposition (SVD) is not required.
4. Approximate inverse of three Kronecker products. The generalized quadratic eigenvalue problem[4] $(\lambda^2 A + \lambda B + C)\nu = 0$ has to be solved. The three matrices can be simultaneously diagonalized if and only if $BA^{-1}C = CA^{-1}B$, which is not satisfied in general.[5] We proceed with the preconditioner as if the condition were satisfied.
5. One-step diagonal scaling on the normal equations. Instead of solving $C\,x = b$, the normal equations $(C^TC)\,x = (C^Tb)$ can be solved to obtain the minimum normal least-squares solution. The matrix (C^TC) is symmetric positive definite but has poor conditioning due to squaring of condition number, $cond(C^TC) = [cond(C)]^2$. A commonly used

preconditioner is just one step of a point Jacobi iteration that is equivalent to a diagonal scaling of (C^TC) to yield 1's on the main diagonal of the preconditioned matrix. The computation required is $x = D^{-1} C^T r$, where D is the diagonal of (C^TC). Note that the diagonal matrix D can be efficiently computed from the Kronecker representation without explicitly forming C^TC or C.

Results and Accomplishments

The original proposal listed three main goals for the project, and each of these has been at least partially accomplished. During the course of this project, it was necessary to completely rewrite the original serial solver because a coding error was uncovered which prevented convergence at low collision frequencies. (Recall that solutions from the serial code were to be used for benchmarking the parallelized code results.) This error was corrected by reformulating the 3-D transport problem using Kronecker products (which was later on useful in the investigation of parallel scaleable methods) *and* by including the particle conservation constraint as an additional block in the tridiagonal structure of the system. Figure 1 shows the diagonal Onsager transport coefficient[6] L_{11} for a low-collision-frequency QPS plasma, calculated for various block sizes corresponding to different numbers of spatial Fourier harmonics. Two versions of the code were run to calculate upper and lower bounds (which converge monotonically with increasing numbers of Fourier modes) as well as a "min-max" extremum whose convergence is not guaranteed to be monotonic. In all cases, it was discovered that the value of the transport coefficient was given quite accurately—even at relatively low numbers of Fourier modes—by the min-max extremum, whereas the rigorous bounds often converged quite slowly and therefore required substantially more computational effort.

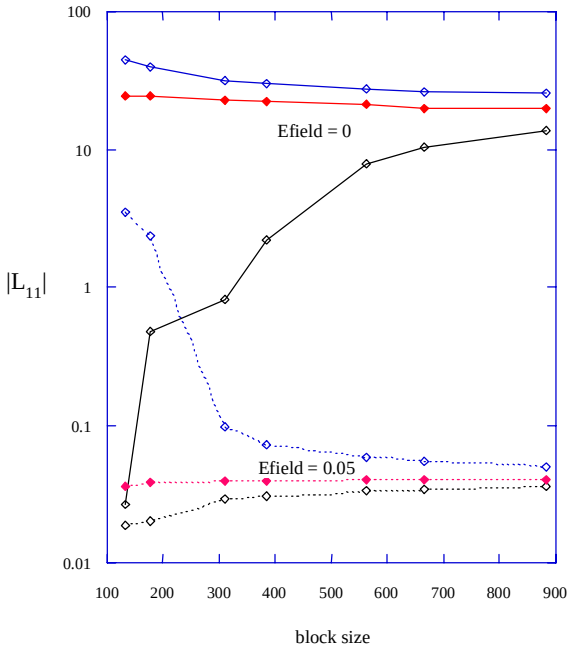

Fig. 1. The diagonal Onsager transport matrix element L_{11} for a QPS plasma in the low-collision-frequency regime and for two values of the radial electric field. The blue (black) curves are upper (lower) bounds, and the red curves are the results of a min-max variational principle.

The first project goal was to investigate the effect of changing the velocity pitch-angle basis functions. At low collision frequencies, sharp boundary layers arise in the pitch angle coordinate between different orbit topologies. The present DKES code uses a Legendre polynomial expansion in the pitch angle, which may not efficiently represent highly localized regions of function variability and therefore requires many modes to adequately approximate these high-gradient boundary layers. The resulting loss of efficiency translates into the need to retain excessively large numbers of basis functions, which exacerbates the "ill-conditioning" of the matrix. We investigated the computational improvements associated with replacing the Legendre basis with different types of basis elements. To consider whether Legendre polynomials are the main cause for poor conditioning, we have considered representations such as Chebyshev polynomials and cubic splines. Although the DKES matrices A_1 arising from a Chebyshev basis are fully dense, this poses no problem storage-wise using the Kronecker representation. Numerical experiments using Chebyshev basis show similar conditioning and eigenvalue distributions as Legendre polynomials and do not seem to be a panacea for the conditioning issues arising from this set of equations.

Another project goal was the development of a scalable iterative solver. This has been achieved with some success for solving large problems (degree=480) on moderately difficult problems ($\nu \sim$ CMUL = 3.1E–3, where ν is the collision frequency normalized to the bounce frequency). The numerical investigations in MATLAB show that the most promising preconditioners are based on the (2) two-term Kronecker products and (5) diagonal scaling of normal equations. Both preconditioners have similar convergence performance but (5) has a simpler implementation. The solver with preconditioner (5) has been implemented using Fortran90 on the IBM SP at CCS/ORNL (Center for Computational Sciences). For moderately difficult problems, the iterative method achieves fast convergence. Table 1 shows the results for 73 Fourier modes. However, for CMUL = 3.1E–5, the iterative method stagnates after about 400 iterations with residual hovering above 1.0E–4. This suggests a more effective physics-based preconditioner is needed for the more challenging low-collisionality case.

Table 1. Normalized ν = 3.1E–3, 73 Fourier modes

Poly degree	Final residual	Time (800 iterations)
60	.8E–14	14 sec
120	.5E–15	38 sec
480	.3E–13	185 sec

Summary and Conclusions

We have developed the framework for future exploration of the preconditioners and associated iterative methods which will be required to extend these calculations to the higher dimensionalities envisioned for future low-collisionality transport analysis of stellarators. We have a better understanding of the challenges, and have taken the initial steps for the development, of a scalable plasma transport code. The preconditioned iterative solver allows the solution for high pitch-angle polynomial degree and for moderately ill-conditioned problems.

This project has benefited the Laboratory in several ways. The acceleration of the 3-D DKES code accomplished in this project has contributed to the successful design of an innovative compact stellarator device QPS which is being proposed for construction at ORNL. The improvements in the existing DKES code will also further enhance ORNL's strength in the worldwide stellarator community. We have begun to address some of the important issues needed to extend this work to higher (4 and 5) dimensions. Further developments of viable preconditioners for this multiscale problem are needed before these relevant stellarator transport problems can be addressed and solved.

The primary funding target for this project (the second round of projects in SciDAC) has been delayed. We do however expect the SciDAC program to continue, and ORNL will be in a better competitive position with the experience of the present work. At the January 2002 3-D theory workshop jointly hosted by ORNL and DOE Office of Fusion Energy Science (OFES), the possibility for a major physics/computational initiative between OFES and OSCAR was discussed. It is our intention to advocate 3-D physics as the focus of this initiative in general and the extensions of DKES to four and five dimensions in particular.

References

[1]S. P. Hirshman et al., "Plasma Transport Coefficients for Nonsymmetric Toroidal Confinement Systems," *Phys. Fluids* **29**, 2951 (1986).

[2]C. Van Loan, "The Ubiquitous Kronecker Product," *Journal of Computational and Applied Mathematics* **123** (1–2): 85–100, Sp. Iss. SI NOV 1 2000.

[3]C. Van Loan and N. Pitsianis, "Approximation with Kronecker Products," pp. 293–314 in *Linear Algebra for Large Scale and Real Time Applications*, ed. M. S. Moonen and G. H. Golub, Kluwer Publications, 1993.

[4]F. Tisseur and K. Meerbergen, "The Quadratic Eigenvalue Problem," *SIAM Review* **43**, 235 (2001).

[5]F. Ma and T. K. Caughey, "Analysis of Linear Nonconservative Vibrations," *Journal of Applied Mechanics* **62**, 685 (1995).

[6]S. P. Hirshman, D. A. Spong, E. D'Azevedo, B. Peyton, and W. Lawkins, "Variational Transport Coefficients for Low Aspect Ratio, Low Collisionality Stellarators," *Bull. Am. Phys. Soc*. **46** (paper, CP1 49, Oct. 2001, Long Beach, CA).

Publication Derived from This Project

S. P. Hirshman, D. A. Spong, E. D'Azevedo, B. Peyton, and W. Lawkins, "Variational Transport Coefficients for Low Aspect Ratio, Low Collisionality Stellarators," *Bull. Am. Phys. Soc*. **46** (paper, CP1 49, Oct. 2001, Long Beach, CA).

Building a Quantum Computer from the Ground Up: Manipulation of the Photoemission of Nanometer-Sized Crystallites via Ultrashort Optical Excitation

R. W. Shaw,[1] C. C. Havener,[2] J. C. Wells,[3] and D. R. Schultz[2]
[1]*Chemical Sciences Division*
[2]*Physics Division*
[3]*Computer Science and Mathematics Division*

Chemically synthesized nanocrystals, as opposed to small numbers of ions confined in elaborate magnetic traps for example, hold the promise of providing a scalable, solid-state pathway towards the creation of a practical quantum computer. Work on this project focuses on producing and controlling the photoemission from the basic building block of such an embodiment: a qubit assembled from semiconductor quantum dots and selectively excited by ultrashort optical pulses.

The coherent creation and manipulation of the excitonic state of a chemically prepared nanocrystal is being explored in order to develop the knowledge necessary to enable the realization of a solid-state qubit, the building block of a quantum computer. Such a device would ultimately operate using manipulation of quantum states rather than classical bits as in conventional computers, opening the possibility of extraordinarily rich computations not conceivable with classical computers and which may speed up many real-world applications such as deciphering encrypted communications. Nanocrystals, as opposed to alternative approaches pursued elsewhere such as small numbers of ions in a magnetic trap or structures fabricated via epitaxy, for example, offer improved size, shape, and electronic property control and a potential for directed assembly. Therefore, nanocrystals hold the promise of opening a pathway to scalable, solid-state quantum computers.

The objectives of the work include observation of the photoluminescence (PL) and photoluminescence excitation (PLE) spectra of various candidate nanocrystal species, determination of the lifetime of these excitonic states as a function of nanocrystal size and temperature, and the creation of superpositions of excitonic states (required for quantum computations).

We have constructed a cryogenic test stand in which we can mount nanocrystals, reduce their temperature using a closed-cycle refrigerator, illuminate them, and observe their emission spectra using a focal plane array detector spectrometer for which new data acquisition and control software was written. The PL spectra of CdSe nanocrystals were obtained at both room temperature and at 10 K. Chromium ion emission lines of the sapphire window of the test stand were used to calibrate and track the sample temperature. Observation was made of the expected temperature shift of the spectra.

We also required semiconductor nanocrystals of another type in order to match the ultrafast laser wavelengths available. Collaboration with Sheng Dai of the Chemical Sciences Division allowed chemical synthesis of InP nanocrystals and, in colloidal suspension, their PL spectra were observed and their size estimated. The need for an ORNL resource such as a proposed nanoscience synthesis center was made clear by our need for, and difficulty in obtaining externally, the appropriate nanoparticles.

We are presently installing two upgrades to our apparatus that will allow us to return to the CdSe nanocrystals that have higher quantum efficiency: (1) a microscope stage cryostat (liquid helium cooled) will allow use of a higher power objective (60×) due to a closer working distance to the nanocrystals and will also eliminate vibrations encountered with the closed-cycle refrigerator, and (2) a supercontinuum-generating tapered fiber optic is being prepared to permit tuning of the ultrafast optical excitation across the CdSe PLE.

The results of our work will lead to proof of concept of our ability to manipulate the quantum state of nanocrystals and enable submission of proposals for follow-on funding to pursue the next steps in the development of a solid-state quantum computer. Already our work has produced a proposal, "Manipulation of semiconductor quantum dots to produce coupled excitonic states for quantum computation," which we have submitted to the U.S. Army Research Office.

Discovering the Quark-Gluon Plasma Using Heavy Quarks

F. E. Barnes and C.-Y. Wong
Physics Division

This project is a theoretical investigation of the interaction of heavy quark mesons with hadron matter. Such calculation are required for the confirmation of the creation of a quark-gluon plasma (QGP) during relativistic heavy-ion collisions. We have carried out cross section calculations for many of the relevant meson-meson processes using both analytical and numerical techniques. These will be used by high-energy heavy-ion collider physicists to investigate the effects of hadronic dissociation collisions on the use of heavy quark suppression as a signal for QGP.

The Relativistic Heavy Ion Collider recently completed at Brookhaven National Laboratory (BNL) has the ultimate goal of producing a QGP, a new type of matter predicted to have existed during the early history of the universe. Recent observations of an anomalous J/ψ suppression in Pb-Pb collisions reported by the NA50 Collaboration indicate that a QGP may have been produced in heavy-ion collisions at CERN, but conclusive evidence is still lacking. Confirmation of the production of a QGP using J/ψ production requires knowledge of the competing J/ψ dissociation in hot hadron matter. Because most of the particles produced in heavy-ion collisions are unstable, the dissociation probability of J/ψ in hadron matter cannot easily be determined experimentally. At present, they are best determined theoretically using well-established models of hadron interactions.

The goal of this project is to understand J/ψ dissociation and its interaction with hadron matter, which will assist the use of J/ψ suppression as a signature for QGP. We are using the well-established constituent-interchange model developed previously by one of us (Barnes) and his collaborator E. S. Swanson [*Phys. Rev. D* **46**, 131 (1992)]. This approach is known to give reasonable agreement with existing experimental low-energy scattering data for a wide range of analogous light hadron-hadron scattering processes. Specifically, we have calculated the dissociation cross sections for J/ψ, ψ′, χ_{cJ}, and Υ mesons in collision with π, *K*, and ρ. A manuscript describing these results has been accepted for publication.[1] T. Barnes and his student N. Black were invited to report on this work at two international meetings in Russia and one in Germany in September 2001. C. Y. Wong was invited to present results on this topic to an international meeting in France in September 2001. In addition, T. Barnes and C. Y. Wong were both invited to visit BNL to report on this topic and to discuss the use of heavy quarks in the discovery of QGP.

Other research topics that we are currently investigating include the cross section for the dissociation of J/ψ in collision with nucleons and the study of the dissociation of a heavy quarkonium as a function of temperature, since the dissociation process depends strongly on the temperature of the hadronic matter. We are examining three ways in which a heavy quarkonium can dissociate at temperatures below the QGP phase transition temperature T_c: spontaneous dissociation, dissociation by thermalization, and dissociation by collision with light hadrons. We are evaluating the dissociation cross sections of π+J/ψ and π+Υ as a function of temperature. We have also found that the dissociation temperatures of all heavy quarkonia, except χ_{b1}, χ_{b2}, and Υ, are below T_c. These results confirm that suppression of J/ψ production by hadron matter is very important, and these hadronic contributions must be understood and incorporated in simulations of heavy-ion collisions before QGP formation can be established through a J/ψ-suppression signature. The results have been submitted for publication in *Physical Review C*.[2]

Regarding follow-on support, we have submitted a proposal to the National Science Foundation in collaboration with E. Swanson of the University of Pittsburgh and H. Crater of The University of Tennessee Space Institute. A proposal to DOE is now in preparation.

Publications Derived from This Project

C. Y. Wong, E. S. Swanson, and T. Barnes, "Heavy Quarkonium Dissociation Cross Sections in Relativistic Heavy-Ion Collisions," *Phys. Rev. C* (in press).

C. Y. Wong, "Dissociation of a Heavy Quarkonium at High Temperatures," LANL Preprint Server nucl-th/0110004.

A Novel Device for Quantitative Single-Atom Detection of ^{14}C

F. W. Meyer
Physics Division

In this project, the feasibility of developing a novel, compact apparatus for the quantitative detection of ^{14}C at a level of about one part in 10^{12} will be investigated. Compounds labeled with ^{14}C are widely used in the pharmaceutical industry (e.g., as tracers to determine the fate of these compounds in vivo). The sensitivities of most present methods are inadequate to permit utilization of sufficiently small quantities of ^{14}C to avoid the issues of radioactive waste and contamination, both of which are unacceptable for environmental, health and safety, and financial reasons. Consequently, the pharmaceutical industry is currently exploring other high-sensitivity ^{14}C detection methodologies that permit reduction of ^{14}C labeling to slightly above background levels. Conventional accelerator mass spectrometry (AMS) is currently the only approach that offers sufficiently high sensitivity to avoid the above radiological issues, but it requires large-scale facilities that are usually not dedicated to a single task, with correspondingly high cost. The AMS technique further entails time-consuming sample preparation prior to the actual measurements and so is not suited to quasi–real time monitoring of ^{14}C levels.

The natural abundance of ^{14}C in "modern" samples is about 1.18×10^{-12} per ^{12}C atom, and this determines the background level from which the levels of tracers used (e.g., in the pharmaceutical industry must be distinguishable). The main difficulty in single atom detection of ^{14}C arises from the isobaric interferences due to atomic ions (e.g., ^{14}N) and molecular ions (e.g., $^{12}CH_2$ and ^{13}CH). In conventional AMS,[1] the approach consists of using a negative ion source to eliminate the ^{14}N contamination, since it does not support a stable negative ion, accelerating the negative ion beam in a tandem accelerator to high energy (few MeV), and then dissociating molecular ions isobaric with $^{14}C^-$, also present in the ion beam, either in a foil or gas target. Subsequent stages of electrostatic and magnetic analysis are then used to isolate the ^{14}C ions before their detection. Conventional AMS requires large facilities, usually not dedicated to a single task, with correspondingly high cost and entails time-consuming sample preparation prior to the actual measurements.

For the present proof-of-principle project, the ORNL Multicharged Ion Research Facility (MIRF)2 electron cyclotron resonance (ECR) ion source will be used for the production of a multicharged carbon beam with charge state of +3 or higher to eliminate molecular isobar interference at mass 14. After magnetic selection of the desired charge state, the multicharged ion beam, which will still be dominated by ^{14}N multicharged ions of the same charge state, is directed at grazing incidence on a metal or insulator single-crystal surface, where efficient negative ion formation takes place without appreciable energy loss of the scattered beams. The different scattered charge states are dispersed with low-resolution electrostatic deflection plates. A second, high-resolution electrostatic analyzer further spatially separates the desired $^{14}C^-$ ions from the other scattered charge states prior to their detection on a two-dimensional position-sensitive detector (2-D PSD). Since ^{14}N does not form a stable negative ion, interference due to ^{14}N is eliminated at the analyzed energy. The neutral ^{14}N scattered beam produces at most an energy independent background on the 2-D PSD and thus may be eliminated by suitable subtraction techniques. Unique characteristics of the apparatus are its small size, low cost, high efficiency (i.e., throughput), and ease of sample preparation, in comparison to conventional AMS hardware. As a result, this apparatus[3] should find great utility in such applications as quasi-real time monitoring of ^{14}C-based chemical tracer uptake in biological systems, atmospheric pollution studies, cancer research, medical diagnostics, and other biomedical studies.

During FY 2001, we have performed a careful analysis of the mass rejection capability of the ORNL MIRF magnetic analysis system. We were able to verify that adjacent mass rejection is more than sufficient to meet the stringent requirements of this project. In addition, the 2D-PSD used in the final stage of ^{14}C detection (i.e., after the negative ion formation by surface scattering) has been extensively refurbished and is being prepared for installation into the surface scattering chamber.

References

[1]D. Elmore and F. M. Philips, Science **236**, 543 (1987).
[2]F. W. Meyer, "ECR-based Atomic Collision Physics Research at ORNL MIRF", in *Trapping Highly_Charged Ions: Fundamentals and Applications,* J. Gillaspy, ed., Nova Science Pub, New York, 2000, pp. 117–164.
[3]F. W. Meyer, "Table-Top Apparatus for Single Atom Detection of Carbon-14," Patent Application No. 09/397, 153, filed Sept. 15, 1999.